Associations of the intestinal microbiome with the complement system in age-related macular degeneration

Denise Corinne Zysset-Burri (denise.zysset@insel.ch)
Inselspital Universitätsklinik für Augenheilkunde https://orcid.org/0000-0002-4147-5374
Irene Keller
Swiss Institute of Bioinformatics
Lieselotte E. Berger
Inselspital Bern Department of Ophthalmology
Carlo R. Largiadèr
Inselspital Bern Department of Clinical Chemistry
Matthias Wittwer
Labor Spiez
Sebastian Wolf
Inselspital Bern Department of Ophthalmology
Martin S. Zinkernagel
Inselspital Bern Department of Ophthalmology

Research

Keywords: age-related macular degeneration, intestinal microbiome, complement system

Posted Date: December 6th, 2019

DOI: https://doi.org/10.21203/rs.2.18334/v1

Abstract

Background: Age-related macular degeneration (AMD) is a leading cause of severe vision loss in the aged population. The etiology of AMD is multifactorial and includes nutritional factors, genetic variants mainly in the complement pathway, environmental risk factors and alterations in the intestinal microbiome. However, it remains largely unexplored whether there is an interdependency of these factors leading to the development of AMD. To investigate this issue, a comprehensive shotgun metagenomics analysis of 57 AMD and 58 healthy controls as well as of 16 complement C3 deficient mice and 16 wildtypes was performed. Single nucleotide polymorphisms (SNPs) in the complement factors were assessed with pre-designed TaqMan® SNP genotyping assays.

Results: The composition of the intestinal microbiome differed significantly between AMD patients and controls. Whereas the class Negativicutes was more abundant in patients, the genus Oscillibacter and Bacteroides species had a significantly higher prevalence in persons without AMD. While SNPs within the complement factor B gene were more abundant in controls, SNPs within the high temperature requirement A serine peptidase 1 and complement factor H (CFH) genes were associated with AMD. Using a classification model, Negativicutes was identified as a potential biomarker for AMD and furthermore, it positively correlated with CFH. In addition, similar taxonomic features were identified that distinguished wildtype mice from C3 deficient mice.

Conclusion: The composition of the intestinal microbiome differs between AMD patients and controls as well as between C3 deficient mice and wildtype mice. Moreover, since the phylum Firmicutes has been identified as potential biomarker for AMD and positively correlates with the genetic risk factor CFH, the study suggests an association between the intestinal microbiome and the complement system in AMD.

Introduction

Age-related macular degeneration (AMD) is the most frequent cause of blindness among older people in developed countries [1]. AMD has become a significant economic and social burden on public health [1] and its prevalence is projected to grow by 50 percent in the next decades [2]. The early stage of AMD results in accumulation of extracellular material underneath the retina, called drusen. Drusen are a sign of impaired retinal pigment epithelium (RPE) function and disruption of the metabolic transport between RPE and choroid [3]. Whereas the intermediate stage of AMD is characterized by larger drusen, the late stages are characterized by either choroidal neovascularization (CNV) in the exudative form or geographic atrophy in the atrophic form of AMD [4]. The pathogenesis of AMD is multifactorial and is thought to be a combination of oxidative stress, impaired RPE function, increased apoptosis and aberrant immune system activation [5].

Despite major research efforts, treatment options for early and intermediate AMD are only very limited. Smoking is the strongest modifiable risk factor for AMD, resulting in oxidative stress, ischemia, hypoxia and ultimately development of CNV. Other environmental risk factors are sunlight exposure [6, 7] and

obesity [8]. To date, the only factor that has been shown to be protective is a healthy diet, rich in omega − 3 fatty acids, lutein, zeaxanthin and antioxidants, consistent with the Age-Related Eye Disease Study 2 (AREDS2) formulation [9]. Therefore, preventative strategies targeting nutritional intake to avoid the development of AMD seem to be most promising [9–14]. Recently we have shown that the composition of the intestinal microbiome may impact AMD development and progression [15]. This link has recently been verified in an animal model, where modifications in the intestinal microbiome have resulted in exacerbation of CNV [16].

In addition to the effect of modifiable environmental risk factors, genetic variants may be associated with AMD such as polymorphisms in complement factor H (CFH) [17]. The discovery of genetic variants in components of the complement system indicated the potential role of local inflammation and complement regulation in the pathogenesis of AMD. Moreover, since toll-like receptors (TLRs) recognize microbe-specific molecules and are expressed on various cells along the gastrointestinal tract, they may be crucial in signaling between the immune system and the microbiota. Moreover, the complement system is a key part of the innate immune system operating via TLR signaling. When over-activated or de-regulated, the complement becomes a major link between infection and inflammation with profound involvement in inflammatory and degenerative diseases such as AMD [18]. In this study, we investigated gut microbiome alterations in patients with AMD and screened for associations between the intestinal microbiome and the complement system.

Results

Taxonomic characterization of the intestinal microbiome in AMD patients and healthy controls

In total, 115 stool samples were sequenced from 57 AMD patients and 58 age- and sex-matched healthy controls. The AMD patients and controls were similar for gender, age at collection, smoking habit and BMI ($p > 0.05$, Table 1). A total of 2.8 billion 100 bp paired-end reads with an average insert size of 350 bp were generated, with an average of 24.3 ± 9.3 (s.d.) million reads per sample. After trimming and filtering, we kept about 2.5 billion non-human high-quality reads, with an average of 21.5 ± 8.5 (s.d.) million reads per sample. The majority of mapped reads were bacterial with 98.8 ± 8.1% (s.d.). The phyla Firmicutes and Bacteroidetes dominated the microbiome composition (Fig. 1). Bacteroidia and Clostridia were the most abundant classes, and Bacteroides, Alistipes and Subdoligranulum the most abundant genera in the cohort, consistent with previous observations [19, 20].

Table 1
Characteristics of study patients

BMI, body mass index; CTRL, control; AMD, age-related macular degeneration.

Data are mean ± SD, $^{\Delta}$ Fisher's exact test, * Welch's t test.

Feature	Patients (n = 57)	Controls (n = 58)	P value AMD vs CTRL
Males (n)	21	25	0.57^{Δ}
Age (years)	75.4 ± 8.3	75.3 ± 8.1	0.92*
Current smoker (n)	6	3	0.31^{Δ}
Previous smoker (n)	20	21	1.0^{Δ}
BMI (kg/m^2)	25.0 ± 4.5	26.0 ± 3.9	0.21*

A previous study has suggested that the human intestinal microbiome can be divided into three enterotypes of distinct microbial composition [19]. To group the AMD patients and control samples into enterotype clusters, we applied the PAM algorithm using Jensen-Shannon distance for relative genus abundances (Fig. 2). The optimal number of enterotypes was three as suggested by the CH index (Fig. 2b). Between-class-analysis was applied to cluster the samples into three enterotypes. (Fig. 2a). The enterotypes were characterized by the following contributors at genus level: Enterotype 1 had a relatively high level of Bacteroides, enterotype 2 of Prevotella and Escherichia was indicative for enterotype 3 (Fig. 2c). However, no association between the enterotypes and the disease status was found ($p > 0.05$, Fisher's exact test), showing an uniform distribution of the samples across the three enterotypes.

A principal component analysis with the health status as grouping variable showed that differences in microbial species abundances separated the patient group from the control group ($p = 0.001$, PERMANOVA analysis with nrepet = 10'000, Fig. 1c). To further examine features of the intestinal microbiome in AMD patients, we compared the relative abundances of taxa between patients and controls, showing that the class Negativicutes was more abundant in patients ($p = 0.0016$) and the genus Oscillibacter ($p = 0.035$) and Bacteroides species ($p = 0.0035$, Wilcoxon rank sum test) were more abundant in controls (Fig. 1D).

Identification of AMD patients based on the intestinal microbiome

To illustrate the potential diagnostic value of the intestinal microbiome for AMD, a species-based classifier was used in an attempt to predict AMD samples among a mixture of samples from patients and healthy controls. Based on the relative species abundance profile from MetaPhlAn, a classification model was constructed using linear shrinkage discriminant analysis and features were ranked according to their correlation adjusted t (cat) scores. A graphical visualization of the cat scores is provided in Fig. 3A. The

blue bars in this figure indicate the ability of a potential biomarker to discriminate between AMD patients and controls in the prediction model. A positive cat score implies that the taxa is over-represented in AMD, whereas a negative score represents an over-represented taxa in controls. The minimum error was reached with seven features (Fig. 3B), which were selected as potential biomarkers, including the class Negativicutes, the order Selenomonadales and the species Phascolarctobacterium, Bacteroides cellulosilyticus, Sutterella wadsworthensis, Bifidobacterium longum and Bacteroides caccae.

Association between single nucleotide polymorphisms and AMD

Out of the genetic polymorphisms previously shown to be associated with risk for AMD [21–34], single nucleotide polymorphisms rs800292 ($p = 0.0012$), rs1410996 ($p = 0.00019$) and rs1061170 ($p = 0.000064$) within the complement factor H (CFH) gene and rs11200638 ($p = 0.00012$) within the high temperature requirement A serine peptidase 1 (HTRA1) gene were associated with a higher risk for having AMD in our cohort. However, rs12614 ($p = 0.0057$) within the complement factor B (CFB) gene was inversely correlated with AMD in the cohort (Fisher's exact test, Table 2).

Table 2
Single nucleotide polymorphisms in AMD

Gene	SNP	A1	A2	F_A1	F_U	P value	OR	95% CI
C2	rs1883025	C	G	0.018	0.052	0.28	0.34	(0.067, 1.72)
C3	rs4420638	C	G	0.25	0.16	0.10	1.74	(0.91, 3.35)
CETP	rs10490924	A	C	0.34	0.35	0.89	0.93	(0.54, 1.61)
CFB1	rs4151667	A	T	0.027	0.052	0.50	0.51	(0.13, 2.11)
CFB2	rs641153	T	C	0.12	0.094	0.67	1.28	(0.55, 2.99)
CFB3	rs12614	A	G	0.027	0.13	0.0057	0.19	(0.053, 0.67)
CFH1	rs800292	A	G	0.24	0.082	0.0012	3.45	(2.31, 5.63)
CFH2	rs1410996	A	G	0.39	0.16	0.00019	3.21	(2.16, 4.85)
CFH3	rs1061170	T	C	0.60	0.34	0.000064	3.03	(1.89, 4.57)
CFI	rs10033900	C	T	0.55	0.45	0.18	1.48	(0.87, 2.50)
COL8A1	rs13095226	C	T	0.13	0.11	0.83	1.16	(0.52, 2.58)
HTRA1	rs11200638	A	G	0.51	0.26	0.00012	2.97	(1.70, 5.20)
LIPC	rs10468017	T	C	0.28	0.29	0.88	0.95	(0.53, 1.68)
TIMP3	rs9621532	C	A	0.0091	0.034	0.37	0.26	(0.028, 2.34)
TNFRSF10A	rs13278062	C	A	0.41	0.5	0.18	0.69	(0.41, 1.17)
VEGF A	rs1413711	T	C	0.47	0.46	0.89	1.07	(0.63, 1.80)

A1, minor allele; A2, major allele; F_A1, frequency of A1 in AMD; F_U, frequency of A1 in controls; OR, odds ratio for A1

Association between the intestinal microbiome and clinical metadata in the cohort

Next, we use multivariate association by linear models (MaAsLin) to examine whether relative abundances of microbial taxa were associated with demographic parameters or with genetic risk factors for AMD (CFH1, CFH2, CFH3 and HTRA1, Fig. 3C). A boosting step in the MaAsLin algorithm ensures that only variables that are associated with the given taxon are included in the linear model, implying that all associations found by the modeling approach have been corrected for all other confounding factors. For demographic parameters, age at collection positively correlated with the species Bacteroides uniformis, Odoribacter unclassified and Eubacterium eligens ($q < 0.2$). There was no association of sex, smoking habit, or BMI with the intestinal microbiome in our cohort ($q > 0.2$). Bacteroides species and

Ruminococcus torques negatively correlated with CFH1 variants, i.e. Bacteroides species and Ruminococcus torques were less abundant in individuals possessing the SNP in the CFH1 gene. The order Clostridiales positively correlated with CFH3 and negatively correlated with CFH1 and CFH2 variants. The class Negativicutes positively correlated with CFH3 (Fig. 3C). There was no association of HTRA1 variants with the intestinal microbiome in the cohort.

Taxonomic characterization of the intestinal microbiome in C3 deficient mice and wildtypes

In total, 64 stool samples were sequenced from 16 $C3^{-/-}$ mice and 16 C57BL/6 control mice (Table 3). A total of 1.9 billion 100 bp paired-end reads with an average insert size of 350 bp were generated, with an average of 31.2 ± 11.1 (s.d.) million reads per sample. After trimming and filtering, we kept about 1.7 billion non-murine high-quality reads, with an average of 27.3 ± 9.9 (s.d.) million reads per sample. The majority of mapped reads were bacterial with 96.8 ± 11.1% (s.d.). The phyla Firmicutes and Bacteroidetes dominated the microbiome composition (Fig. 4A) in accordance with previous observations [35].

Table 3
Parameters of Animal experiments

Experimental group	Mouse	Timepoints (weeks)	Sex (m/w)	Number of mice
1	B6;129S4-$C3^{tm1Crr}$/J	1 + 4	m	8
2	B6;129S4-$C3^{tm1Crr}$/J	1 + 4	f	8
3	C57BL/6J	1 + 4	m	8
4	C57BL/6J	1 + 4	f	8 (6)

Two wildtype males were euthanized due to fighting activites before stool sampling have been performed at week 4. B6;129S4-$C3^{tm1Crr}$/J, complement factor C3-deficient mice; C57BL/6J, wildtypes.

A principal component analysis showed that differences in microbial species abundances separated the $C3^{-/-}$ mice from the wildtypes ($p = 0.001$, PERMANOVA analysis with nrepet = 10000, Fig. 4C). To further examine features of the intestinal microbiome in $C3^{-/-}$ mice, we compared the relative abundances of taxa between C3 deficient mice and wildtypes, showing that the phylum Firmicutes was more abundant in $C3^{-/-}$ mice ($p < 0.0001$) and the phylum Bacteroidetes was more abundant in wildtypes ($p < 0.0001$; Fig. 4D). There was no association of sex or week at collection with the intestinal microbiome in the cohort ($q > 0.02$).

Discussion

Despite advances in the treatment of neovascular AMD, effective preventative strategies of this disease are lacking. An association of diet with development of advanced AMD has been shown in various studies (AREDS I and II). In this study, we investigated associations between the intestinal microbiome and the complement system in AMD. Microbiota in AMD patients and healthy controls was analyzed in terms of taxonomic profile and correlated to clinical metadata and genetic risk factors including SNPs in genes encoding for complement factors. We identified several taxonomic units of the intestinal microbiome that differ between patients and healthy controls in their relative abundance, suggesting that they may be associated with the development of AMD. The genus Oscillibacter and Bacteroides species were more abundant in healthy controls relative to AMD patients. In contrast, the class Negativicutes was more abundant in AMD patients compared to controls. These results are consistent with previous studies, reporting associations between several of these species and AMD, [15, 36].

After smoking, obesity is the second most important environmental risk factor for AMD [37]. Numerous studies have shown that a higher relative abundance of Firmicutes and a lower Bacteroidetes abundance are typically associated with obesity [38]. In a previous study, we observed a shift of relative abundance in Firmicutes at the expense of Bacteroidetes in AMD patients [15]. In this study, the class Negativicutes belonging to the phylum Firmicutes was enriched in AMD patients. Moreover, Bacteroides species belonging to the phylum Bacteroidetes was more abundant in controls. Looking at the prediction model in Fig. 3A, Negativicutes as well as the order Selenomonadales, both belonging to the phylum Firmicutes, may be identified as potential biomarkers for AMD. On the other hand, Bacteroides species, especially including B. cellulosilyticus and B. caccae, may have a protective effect on the development of AMD as these species were more abundant in the control group. Taken together, these results suggest an elevated Firmicutes to Bacteroidetes ratio, also at lower taxonomic levels in AMD patients compared to healthy controls. These data are also consistent with observations in mice, demonstrating that high-fat diets exacerbate choroidal neovascularization, which is a hallmark of exudative AMD, by increasing the relative abundance of Firmicutes [36].

In addition to environmental risk factors, genetic risk factors mostly associated with the complement system are involved in the development of AMD. The first genome-wide association study for AMD performed in 2005 identified a highly associated genetic variant in complement factor H (CFH) [39]. This genetic link between AMD and the complement system was further expanded by several studies showing an association between other complement factors such as complement component 3 (C3), complement component C2 (C2) and complement factor B (CFB) [40, 41]. In our cohort, while single nucleotide polymorphisms (SNPs) within the CFH gene are associated with a higher risk for developing AMD, SNP within the CFB gene has a protective effect (Table 2). Furthermore, to assess associations between the complement system and the intestinal microbiome, both involved into the development of AMD, microbiota of C3 deficient mice and wildtypes was analyzed in terms of taxonomic profile and correlated to clinical metadata. While the phylum Firmicutes was more abundant, the phyla Bacteroidetes was decreased in C3 deficient mice compared to wildtypes (Fig. 4). Since Firmicutes was proposed as potential biomarker for AMD, it may also contribute to the development of AMD in C3 deficient mice. These results show that the complement alters the intestinal microbiota composition in mice and as such

microbiota-derived nutrients, metabolites and antigens within the host. This in turn may promote degenerative diseases such as AMD. This association between the complement system and the intestinal microbiome was further confirmed in humans by the correlation of SNPs within the CFH gene with the taxa Negativicutes, Clostridiales, Bacteroides species, and Ruminococcus torques (Fig. 3C). Complement factor H is the soluble inhibitor of the alternative pathway of complement, mediating anti-inflammatory housekeeping functions by protecting cells from complement activation. Thus, mutations in the CFH gene result in uncontrolled complement activation, which is involved in the pathogenesis of AMD [42]. Since Negativicutes, which was proposed as potential biomarker for AMD (Fig. 3A), positively correlated with CFH, it may influence the development and/or progression of AMD via the regulation of the alternative pathway of complement. Moreover, while the relative abundance of Bacteroides species were proposed as potential biomarker for controls and negatively correlated with CFH, they may be protective for AMD.

Limitations of this study include the lack of longitudinal data and the limited number of patients.

Conclusions

In conclusion, we found alterations of the intestinal microbiome in AMD patients. While the phylum Firmicutes was more abundant in patients with AMD, Bacteroides species may be protective for AMD, both correlating with the genetic risk factor CFH. This data points towards a possible interconnection between the intestinal microbiome, the complement system and the development of AMD. However, the data do not allow to determine whether the altered intestinal microbiome is the consequence of the disease or is involved in its pathogenesis via uncontrolled activation of the complement system.

Methods

Study design and recruitment

Participants (n = 115) were recruited from the Department of Ophthalmology of the University Hospital Bern (Inselspital), Switzerland. The study was conducted in accordance with the Declaration of Helsinki and approved by the Ethics Committee of the Canton of Bern (ClinicalTrials.gov: NCT02438111). After receiving oral and written information, all participants gave written informed consent to participate in the study. All participants were subjected to an ophthalmic examination including optical coherence tomography and standard fundus color photography. Patients (n = 57) had clinically confirmed AMD and were 50 years of age or older, and the control group (n = 58) was selected to represent an age- and sex-matched group with no signs of AMD. Exclusion criteria for both groups were chronic inflammatory or gastrointestinal diseases (including previous surgery in the gastrointestinal tract) and use of systemic antibiotics within the last three months.

Metagenomic DNA sequencing and annotation

Stool samples were provided refrigerated to the study center within 16 hours after fecal output where they were immediately frozen at -20 °C. Metagenomic DNA was isolated from up to 200 mg of stool sample using the PSP® Spin Stool DNA Plus kit (Stratec Biomedical AG, Beringen, Switzerland) according to the manufacturer's protocol with an integrated RNA digestion step using 100 mg/ml RNase A (Qiagen, Hombrechtikon, Switzerland). All samples were sequenced on the Illumina HiSeq 3000 platform with up to ten samples pooled in one lane (Next Generation Sequencing Platform of the Unviersity of Bern, Switzerland). To exclude low-quality reads and reads mapping to human DNA, the resulting 150 bp paired-end reads were quality filtered with Trimmomatic v.0.32 [43] and mapped to the human reference genome hg19 using Bowtie2 v.2.2.4 [44]. For taxonomical analysis, the high-quality non-human reads were mapped against a set of clade-specific marker sequences using the Metagenomic Phylogenetic Analysis tool v.2.6.0 (MetaPhlAn2) and the marker database v.20 [45] using default settings. In order to provide the relative abundance of each taxonomic unit, Bowtie2 v.2.2.4 was applied for alignment followed by normalization of the total number of reads in each clade by the nucleotide length of its marker.

Genetic analysis of germline DNA

Genomic DNA was extracted from EDTA blood samples using a QIAamp DNA Blood Midi Kit (Qiagen AG, Basel, Switzerland). To identify genetic risk factors for AMD, 16 previously described SNPs were analyzed (supplementary Table 1). Real-time quantitative PCR (see below) was used for allelic discrimination of all SNPs analysed except for CFB (rs4151667, rs12614 and rs641153) which was assessed by Sanger sequencing. This locus was amplified using the Multiplex PCR Kit (Qiagen, Hombrechtikon, Switzerland) with an initial 15 min denaturation step at 95 °C, followed by 35 amplification cycles (30 s at 94 °C, 90 s at 58 °C, 60 s 72 °C) and a final 10 min extension at 72 °C. The following forward and reverse primers were used: 5'-GGTCTAGGTCTGGAGTTTCAGC-3' and 5'- TTGGTCTTGAGTCTTCAGGGTG-3. PCR products were purified using the QIAquick PCR Purification Kit (Qiagen) and Sanger sequenced using the same primers as used for PCR amplification. Bi-directional sequencing was performed with the BigDye® Terminator v3.1 Cycle Sequencing Kit (Life Technologies, Zug, Switzerland) on a 3130xl Genetic Analyzer. Cycle Sequencing was carried out with an initial 1 min denaturation at 96 °C, followed by 25 amplification cycles (10 s at 96 °C, 5 s at 50 °C, 75 s 60 °C). Sequences were aligned and compared to the reference sequences (NG_008191.1 and NC_000006.12) using the Sequencer 5.0 software (Gene Codes Corporation, Ann Arbor, USA).

Pre-designed TaqMan® SNP genotyping assays (Applied Biosystems, Foster City, CA, USA) were obtained for rs4420638, rs1061170, and rs13278062. Custom designed TaqMan® assays (Assay-by-Design, Applied Biosystems) were obtained for all other SNPs. Allelic discrimination was performed on a 7500 Fast Real-Time PCR System (Applied Biosystems) according to the manufacturer's protocol.

Enterotyping

The samples were clustered based on relative genus abundances using Jensen-Shannon distance and the partitioning around medoids (PAM) algorithm. The optimal number of clusters was calculated by the

Calinski-Harabasz (CH) index. Between-class-analysis (BCA), a particular case of principal component analysis (PCA), was used to visualize the taxonomic drivers of the clusters [19].

Statistical Analysis

Demographics were compared among groups using either Welch's t test (for age and BMI) or Fisher's exact test (for sex and smoking, Table 1). The Wilcoxon rank sum test was used to identify significant differences in microbial abundances. To detect an association between enterotypes and the disease status, Fisher's exact test was applied in GraphPad Prism version 7.04 (GraphPad software Inc.). P-values < 0.05 were considered to be significant.

The association analyses between AMD and the SNPs were conducted using Fisher's exact test implemented in PLINK v.1.07 [46]. For subsequent analysis, genotypes at each locus of each individual are coded as follows: 0 for major allele homozygous, 1 for heterozygous and 2 for minor allele homozygous.

R software (version 3.5.1) was used to perform other analyses. The R package ade4 [47] was used to perform PCA providing global analysis of microbial abundances between groups. PCA was performed with scaled values on relative abundances of microbial species identified by MetaPhlAn2. A visualization of the individual samples grouped by case and control is provided in Figs. 1C and 4C. Permutation multivariate analysis of variance (PERMANOVA) using the R package vegan [48] was assessed with 1000 permutations to calculate a p value for separation. Associations of microbial abundances with clinical metadata were analyzed using multivariate association by linear models (MaAsLin) [49] R package. Significant association was considered below a q value threshold of 0.20 after adjusting for false discovery rate (FDR; Benjamini Hochberg). For clinical metadata, the R package corrplot was used for visualization of the data in a correlation matrix (Fig. 3B). The R package sda provided the functionality for high-dimensional linear discriminant analysis with feature selection. A species-based classifier using the relative species abundance profile from MetaPhlAn was trained using Stein-type shrinkage estimators and features are ranked according to correlation-adjusted t (cat) scores to provide a set of candidate biomarkers (Fig. 3A). The minimum error was calculated by 100-fold cross-validation by the "rfcv" function of the randomForest package with sequentially reduced numbers of features. The optimal number of features was selected by cross-validation. The model was tested on the testing set using this set of features and a receiver operating (ROC) curve within the pROC package in R.

Mice

Adult (6–8 weeks of age) $C3^{-/-}$ mice on a C57BL/6 background (B6;129S4-$C3^{tm1Crr}$ /J, n = 16) and C57BL/6 mice as controls (n = 16), both from Jackson Laboratory (Bar Harbor, ME, USA), were used for this study. Mice were housed in groups of 4 animals of the same gender under temperature and humidity-controlled conditions in individually ventilated cages giving sterile food and water ad libitum and exposed to 12:12 h light:dark cycles. One and 4 weeks after arrival of the mice, faeces were collected and immediately frozen at -20 °C. At the end of the study, mice were euthanized by carbon dioxide (CO_2)

inhalation. Metagenomic DNA was isolated and sequenced as described above. To exclude low-quality reads and reads mapping to murine DNA, the resulting 150 bp paired-end reads were quality filtered with Trimmomatic v.0.32 [43] and mapped to the mouse reference genome GRCm38 using Bowtie2 v.2.3.0 [44]. The high-quality non-murine reads were taxonomically profiled using MetaPhlAn2, and associations of microbial abundances with genetics ($C3^{-/-}$ versus wildtype mice) and demographic parameters (sex and week at collection) were identified by MaAsLin (for details see above). All animal studies were conducted at the University of Bern and approved by the local Animal Ethics Committee (Veterinärdienst des Kantons Bern / BE99-16).

Declarations

Ethics approval and consent to participate

This study was approved by the Ethics Committee of the Canton of Bern (ClinicalTrials.gov: NCT02438111) and all participants gave written informed consent to participate in the study.

All animal studies were approved by the local Animal Ethics Committee (Veterinärdienst des Kantons Bern / BE99-16).

Consent for publication

Not applicable.

Availability of data and material

The datasets supporting the conclusions of this article are available in the European Nucleotide Archive under accession numbers PRJEB24557 and PRJEB35615.

Competing interests

The authors declare that they have no competing financial interests.

Funding

Not applicable.

Author's contribution

D.C.Z., M.S.Z. and S.W. conceived and designed the project. D.C.Z. and C.R.L. performed the experiments. D.C.Z., I.K. and M.W. analyzed the sequencing data. M.S.Z. and L.E.B. examined the study subjects. All authors contributed writing and editing the manuscript.

Acknowledgements

Not applicable.

References

1. Friedman DS, O'Colmain BJ, Munoz B, Tomany SC, McCarty C, de Jong PT, Nemesure B, Mitchell P, Kempen J, Eye Diseases Prevalence Research G: Prevalence of age-related macular degeneration in the United States. Arch Ophthalmol 2004, 122:564-572.
2. Wong WL, Su X, Li X, Cheung CM, Klein R, Cheng CY, Wong TY: Global prevalence of age-related macular degeneration and disease burden projection for 2020 and 2040: a systematic review and meta-analysis. Lancet Glob Health 2014, 2:e106-116.
3. Sarks S, Cherepanoff S, Killingsworth M, Sarks J: Relationship of Basal laminar deposit and membranous debris to the clinical presentation of early age-related macular degeneration. Invest Ophthalmol Vis Sci 2007, 48:968-977.
4. Ambati J, Fowler BJ: Mechanisms of age-related macular degeneration. Neuron 2012, 75:26-39.
5. Seddon JM, George S, Rosner B: Cigarette smoking, fish consumption, omega-3 fatty acid intake, and associations with age-related macular degeneration: the US Twin Study of Age-Related Macular Degeneration. Arch Ophthalmol 2006, 124:995-1001.
6. Tomany SC, Cruickshanks KJ, Klein R, Klein BE, Knudtson MD: Sunlight and the 10-year incidence of age-related maculopathy: the Beaver Dam Eye Study. Arch Ophthalmol 2004, 122:750-757.
7. Tomany SC, Klein R, Klein BE, Beaver Dam Eye S: The relationship between iris color, hair color, and skin sun sensitivity and the 10-year incidence of age-related maculopathy: the Beaver Dam Eye Study. Ophthalmology 2003, 110:1526-1533.
8. Seddon JM, Cote J, Rosner B: Progression of age-related macular degeneration: association with dietary fat, transunsaturated fat, nuts, and fish intake. Arch Ophthalmol 2003, 121:1728-1737.
9. Chew EY, Clemons TE, Agron E, Launer LJ, Grodstein F, Bernstein PS, Age-Related Eye Disease Study 2 Research G: Effect of Omega-3 Fatty Acids, Lutein/Zeaxanthin, or Other Nutrient Supplementation on Cognitive Function: The AREDS2 Randomized Clinical Trial. JAMA 2015, 314:791-801.
10. Age-Related Eye Disease Study Research G, SanGiovanni JP, Chew EY, Clemons TE, Ferris FL, 3rd, Gensler G, Lindblad AS, Milton RC, Seddon JM, Sperduto RD: The relationship of dietary carotenoid and vitamin A, E, and C intake with age-related macular degeneration in a case-control study: AREDS Report No. 22. Arch Ophthalmol 2007, 125:1225-1232.
11. Ersoy L, Ristau T, Lechanteur YT, Hahn M, Hoyng CB, Kirchhof B, den Hollander AI, Fauser S: Nutritional risk factors for age-related macular degeneration. Biomed Res Int 2014, 2014:413150.
12. SanGiovanni JP, Chew EY, Clemons TE, Davis MD, Ferris FL, 3rd, Gensler GR, Kurinij N, Lindblad AS, Milton RC, Seddon JM, et al: The relationship of dietary lipid intake and age-related macular degeneration in a case-control study: AREDS Report No. 20. Arch Ophthalmol 2007, 125:671-679.
13. Seddon JM: Multivitamin-multimineral supplements and eye disease: age-related macular degeneration and cataract. Am J Clin Nutr 2007, 85:304S-307S.
14. Seddon JM, Ajani UA, Sperduto RD, Hiller R, Blair N, Burton TC, Farber MD, Gragoudas ES, Haller J, Miller DT, et al.: Dietary carotenoids, vitamins A, C, and E, and advanced age-related macular degeneration. Eye Disease Case-Control Study Group. JAMA 1994, 272:1413-1420.
15. Zinkernagel MS, Zysset-Burri DC, Keller I, Berger LE, Leichtle AB, Largiader CR, Fiedler GM, Wolf S:

Association of the Intestinal Microbiome with the Development of Neovascular Age-Related Macular Degeneration. Sci Rep 2017, 7:40826.
16. Andriessen EM, Wilson AM, Mawambo G, Dejda A, Miloudi K, Sennlaub F, Sapieha P: Gut microbiota influences pathological angiogenesis in obesity-driven choroidal neovascularization. EMBO Mol Med 2016.
17. Maller J, George S, Purcell S, Fagerness J, Altshuler D, Daly MJ, Seddon JM: Common variation in three genes, including a noncoding variant in CFH, strongly influences risk of age-related macular degeneration. Nat Genet 2006, 38:1055-1059.
18. Chen M, Xu H: Parainflammation, chronic inflammation, and age-related macular degeneration. J Leukoc Biol 2015, 98:713-725.
19. Arumugam M, Raes J, Pelletier E, Le Paslier D, Yamada T, Mende DR, Fernandes GR, Tap J, Bruls T, Batto JM, et al: Enterotypes of the human gut microbiome. Nature 2011, 473:174-180.
20. Tap J, Mondot S, Levenez F, Pelletier E, Caron C, Furet JP, Ugarte E, Munoz-Tamayo R, Paslier DL, Nalin R, et al: Towards the human intestinal microbiota phylogenetic core. Environ Microbiol 2009, 11:2574-2584.
21. Edwards AO, Ritter R, 3rd, Abel KJ, Manning A, Panhuysen C, Farrer LA: Complement factor H polymorphism and age-related macular degeneration. Science 2005, 308:421-424.
22. Fritsche LG, Loenhardt T, Janssen A, Fisher SA, Rivera A, Keilhauer CN, Weber BH: Age-related macular degeneration is associated with an unstable ARMS2 (LOC387715) mRNA. Nat Genet 2008, 40:892-896.
23. Hirata FE, de Vasconcellos JP, Medina FM, Rim PH, Fulco EA, de Melo MB: Association of LOC387715/ARMS2 (rs10490924) Gene Polymorphism with Age-Related Macular Degeneration in the Brazilian Population. Ophthalmic Genet 2015, 36:224-228.
24. Liu K, Chen LJ, Lai TY, Tam PO, Ho M, Chiang SW, Liu DT, Young AL, Yang Z, Pang CP: Genes in the high-density lipoprotein metabolic pathway in age-related macular degeneration and polypoidal choroidal vasculopathy. Ophthalmology 2014, 121:911-916.
25. Merle BM, Maubaret C, Korobelnik JF, Delyfer MN, Rougier MB, Lambert JC, Amouyel P, Malet F, Le Goff M, Dartigues JF, et al: Association of HDL-related loci with age-related macular degeneration and plasma lutein and zeaxanthin: the Alienor study. PLoS One 2013, 8:e79848.
26. Richardson AJ, Islam FM, Aung KZ, Guymer RH, Baird PN: An intergenic region between the tagSNP rs3793917 and rs11200638 in the HTRA1 gene indicates association with age-related macular degeneration. Invest Ophthalmol Vis Sci 2010, 51:4932-4936.
27. Richardson AJ, Islam FM, Guymer RH, Baird PN: Analysis of rare variants in the complement component 2 (C2) and factor B (BF) genes refine association for age-related macular degeneration (AMD). Invest Ophthalmol Vis Sci 2009, 50:540-543.
28. Sun Y, Li S, Li H, Yang F, Bai Y, Zhao M, Guo J, Zhao M, Zhou P, Khor CC, et al: TNFRSF10A-LOC389641 rs13278062 but not REST-C4orf14-POLR2B-IGFBP7 rs1713985 was found associated with age-related macular degeneration in a Chinese population. Invest Ophthalmol Vis Sci 2013, 54:8199-8203.
29. Wang X, Zhang Y, Zhang MN: Complement factor B polymorphism (rs641153) and susceptibility to age-related macular degeneration: evidence from published studies. Int J Ophthalmol 2013, 6:861-867.
30. Wang Y, Wang M, Han Y, Zhang R, Ma L: ABCA1 rs1883025 polymorphism and risk of age-related

macular degeneration. Graefes Arch Clin Exp Ophthalmol 2016, 254:323-332.
31. Wu PB, Gu H, Yang XF, Liu NP: [Association of single nucleotide polymorphism in complement factor I gene with age-related macular degeneration]. Zhonghua Yan Ke Za Zhi 2013, 49:350-356.
32. Yu Y, Huang L, Wang B, Zhang C, Bai Y, Li X: COL8A1 rs13095226 polymorphism shows no association with neovascular age-related macular degeneration or polypoidal choroidal vasculopathy in Chinese subjects. Int J Clin Exp Pathol 2015, 8:11635-11640.
33. Zeng R, Wen F, Zhang X, Zuo C, Li M, Chen H, Wu K: An rs9621532 variant near the TIMP3 gene is not associated with neovascular age-related macular degeneration and polypoidal choroidal vasculopathy in a Chinese Han population. Ophthalmic Genet 2012, 33:139-143.
34. Zhang MX, Zhao XF, Ren YC, Geng TT, Yang H, Feng T, Jin TB, Chen C: Association between a functional genetic polymorphism (rs2230199) and age-related macular degeneration risk: a meta-analysis. Genet Mol Res 2015, 14:12567-12576.
35. Ley RE, Turnbaugh PJ, Klein S, Gordon JI: Microbial ecology: human gut microbes associated with obesity. Nature 2006, 444:1022-1023.
36. Andriessen EM, Wilson AM, Mawambo G, Dejda A, Miloudi K, Sennlaub F, Sapieha P: Gut microbiota influences pathological angiogenesis in obesity-driven choroidal neovascularization. EMBO Mol Med 2016, 8:1366-1379.
37. Adams MK, Simpson JA, Aung KZ, Makeyeva GA, Giles GG, English DR, Hopper J, Guymer RH, Baird PN, Robman LD: Abdominal obesity and age-related macular degeneration. Am J Epidemiol 2011, 173:1246-1255.
38. Mathur R, Barlow GM: Obesity and the microbiome. Expert Rev Gastroenterol Hepatol 2015, 9:1087-1099.
39. Klein RJ, Zeiss C, Chew EY, Tsai JY, Sackler RS, Haynes C, Henning AK, SanGiovanni JP, Mane SM, Mayne ST, et al: Complement factor H polymorphism in age-related macular degeneration. Science 2005, 308:385-389.
40. Gold B, Merriam JE, Zernant J, Hancox LS, Taiber AJ, Gehrs K, Cramer K, Neel J, Bergeron J, Barile GR, et al: Variation in factor B (BF) and complement component 2 (C2) genes is associated with age-related macular degeneration. Nat Genet 2006, 38:458-462.
41. Maller JB, Fagerness JA, Reynolds RC, Neale BM, Daly MJ, Seddon JM: Variation in complement factor 3 is associated with risk of age-related macular degeneration. Nat Genet 2007, 39:1200-1201.
42. Toomey CB, Johnson LV, Bowes Rickman C: Complement factor H in AMD: Bridging genetic associations and pathobiology. Prog Retin Eye Res 2018, 62:38-57.
43. Bolger AM, Lohse M, Usadel B: Trimmomatic: a flexible trimmer for Illumina sequence data. Bioinformatics 2014, 30:2114-2120.
44. Langmead B, Salzberg SL: Fast gapped-read alignment with Bowtie 2. Nat Methods 2012, 9:357-359.
45. Segata N, Waldron L, Ballarini A, Narasimhan V, Jousson O, Huttenhower C: Metagenomic microbial community profiling using unique clade-specific marker genes. Nat Methods 2012, 9:811-814.
46. Purcell S, Neale B, Todd-Brown K, Thomas L, Ferreira MA, Bender D, Maller J, Sklar P, de Bakker PI, Daly MJ, Sham PC: PLINK: a tool set for whole-genome association and population-based linkage analyses. Am J Hum Genet 2007, 81:559-575.

47. Stéphane Dray A-BeD: The ade4 Package: Implementing the Duality Diagram for Ecologists. Journal of Statistical Software 2007, 22.
48. Anderson MJ: A new method for non-parametric multivariate analysis of variance. Austral Ecology 2001, 26:32-46.
49. Morgan XC, Tickle TL, Sokol H, Gevers D, Devaney KL, Ward DV, Reyes JA, Shah SA, LeLeiko N, Snapper SB, et al: Dysfunction of the intestinal microbiome in inflammatory bowel disease and treatment. Genome Biol 2012, 13:R79.

Additional Files

Additional file 1. Single nucleotide polymorphisms in AMD

Additional file 1.docx

Trial Registration

ClinicalTrials.gov: NCT02438111. Registered 08 May 2015 - https://clinicaltrials.gov

Figures

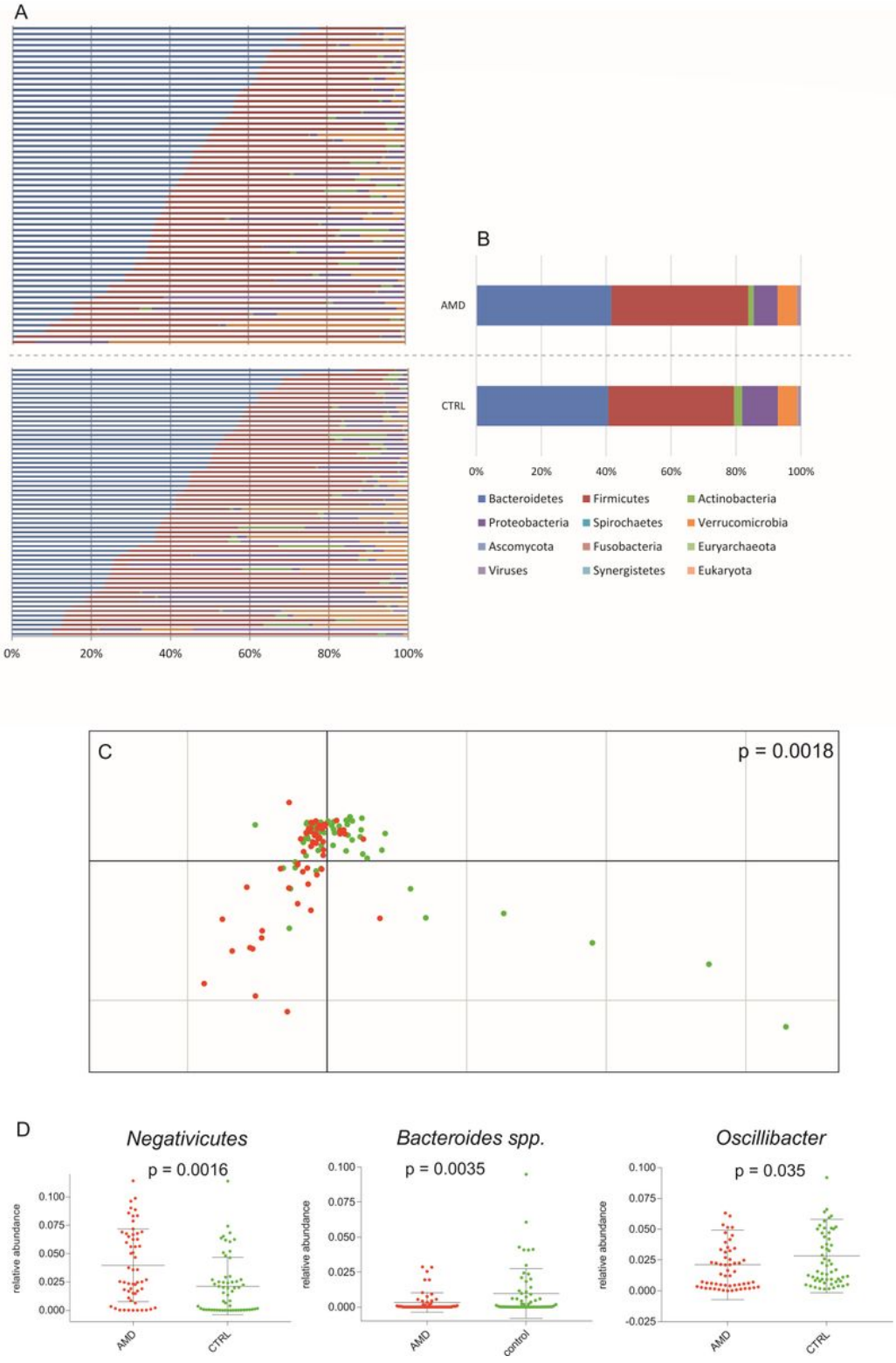

Figure 1

Diversity of the intestinal microbiome in AMD patients and healthy controls. Relative abundances of microbiota at phyla level in all study subjects (a) and averaged for study groups (b). c: Principal component analysis of microbial species abundance grouped patients and controls separately, with PERMANOVA confirming a significant difference between the groups ($p = 0.0018$). d: Relative abundances of taxa associated with AMD (Wilcoxon rank sum test, $p < 0.05$).

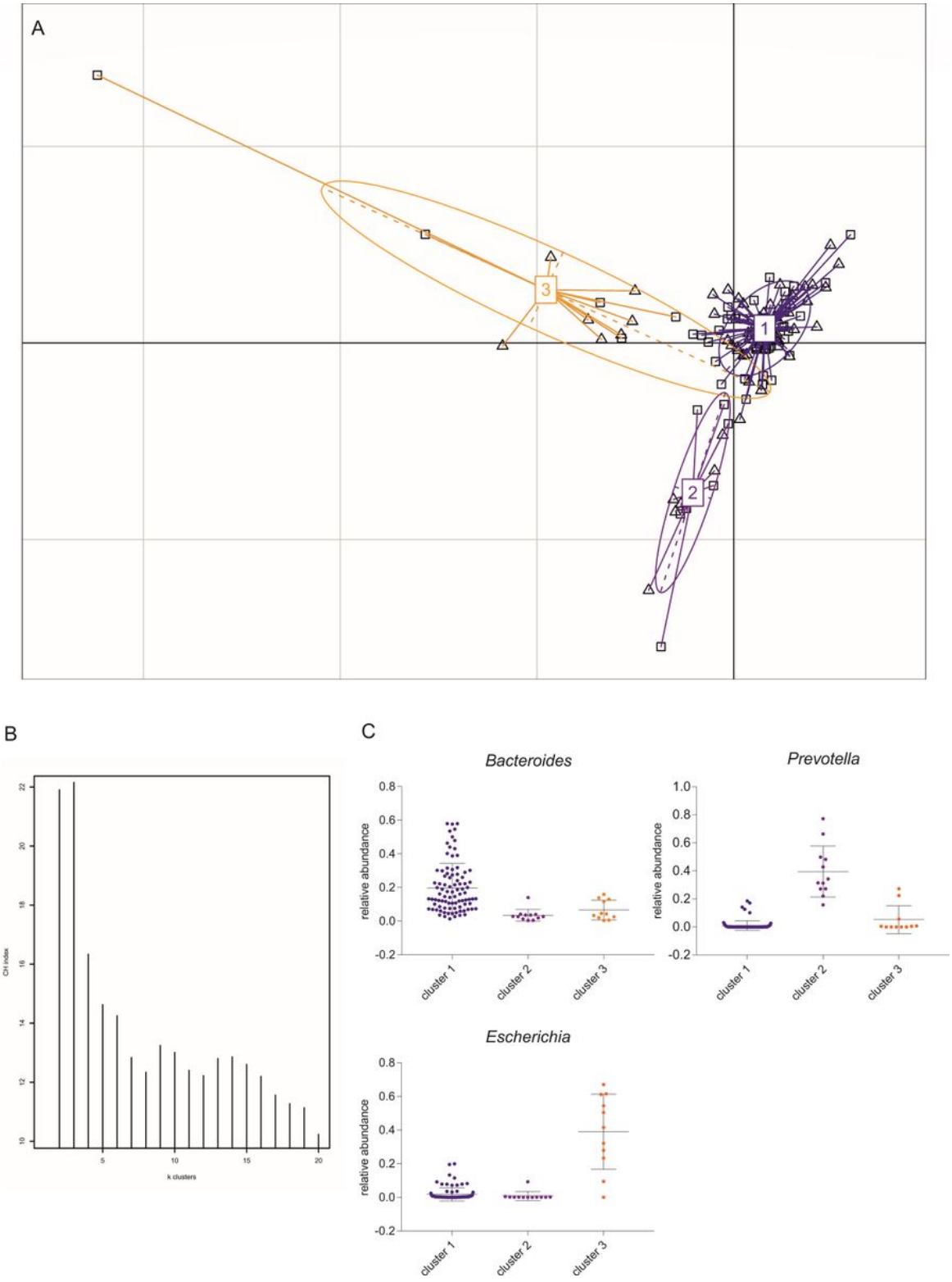

Figure 2

Enterotypes of the intestinal microbiome in AMD patients and healthy controls. a: The intestinal microbiota was clustered into three enterotypes at genus level, dominated by Bacteroides (enterotype 1), Prevotella (enterotype 2) and Escherichia (enterotype 3). Patients (n=57) and controls (n=58) were denoted by squares (□) and triangles (Δ), respectively. b: The optimal number of enterotypes was three as indicated by the maximum Calinski-Harabasz (CH) index at three clusters. c: Relative abundances of

the dominant genera in the three enterotypes. Blue is enterotype 1, purple is enterotype 2 and orange is enterotype 3.

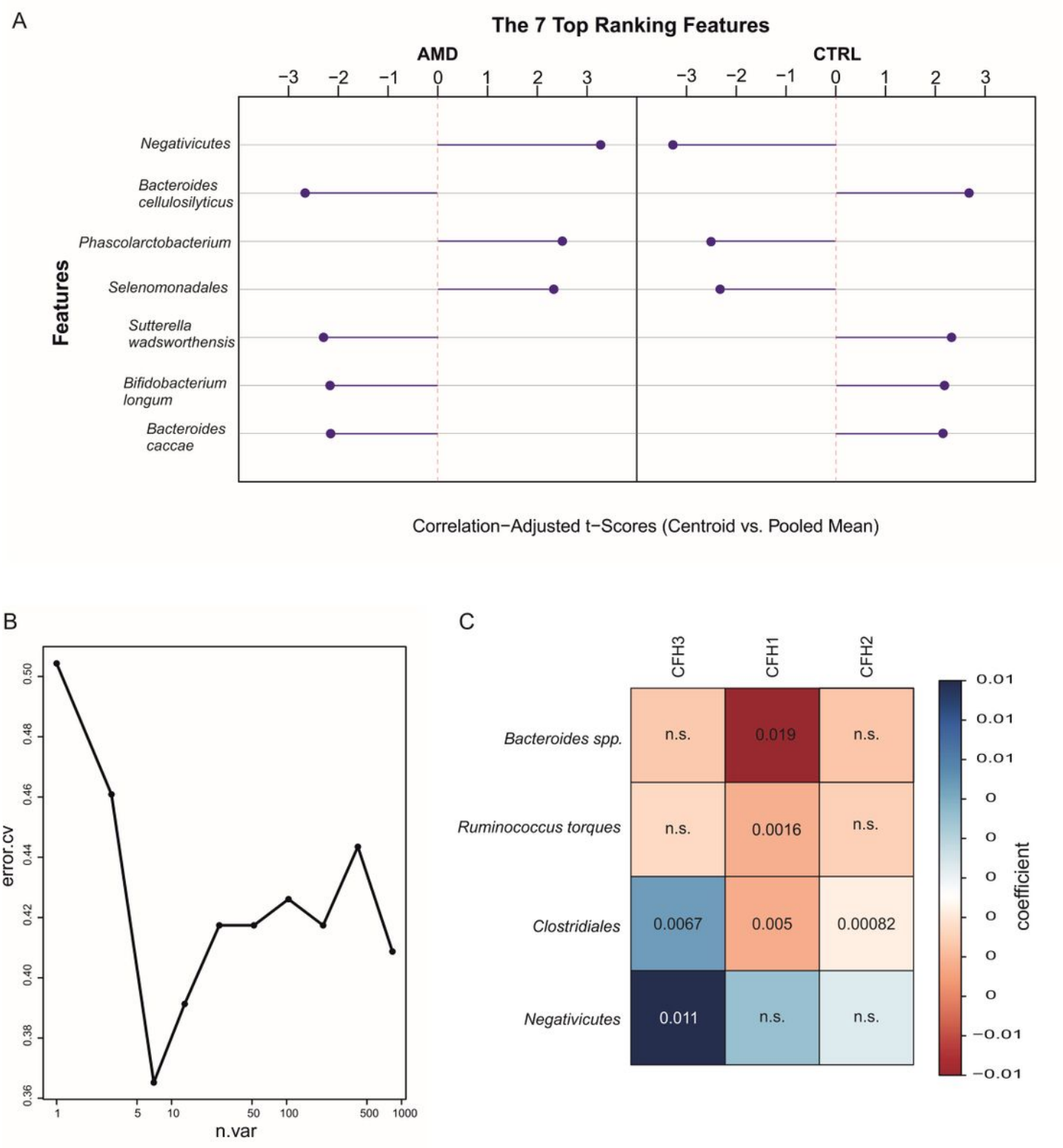

Figure 3

Classification to differentiate samples between AMD patients and healthy controls. a: List of the top 7 ranked biomarkers for AMD. Ranking was performed on correlation adjusted t (cat) scores. The length and direction of the blue bars indicated the influence of a given biomarker on the discriminative power of

the prediction model. The class Negativicutes had the highest potential for the separation of AMD patients and healthy controls with a positive cat score indicating an over-representation in patients. b: Cross-validation with sequentially reduced number of predictors indicated that the prediction error was minimized at seven features. c: Correlation between microbial taxa and clinical metadata. R-coefficients and corresponding p-values from MaAsLin are shown. Coefficients are indicated using a color gradient. Red indicates negative correlation, blue positive correlation.

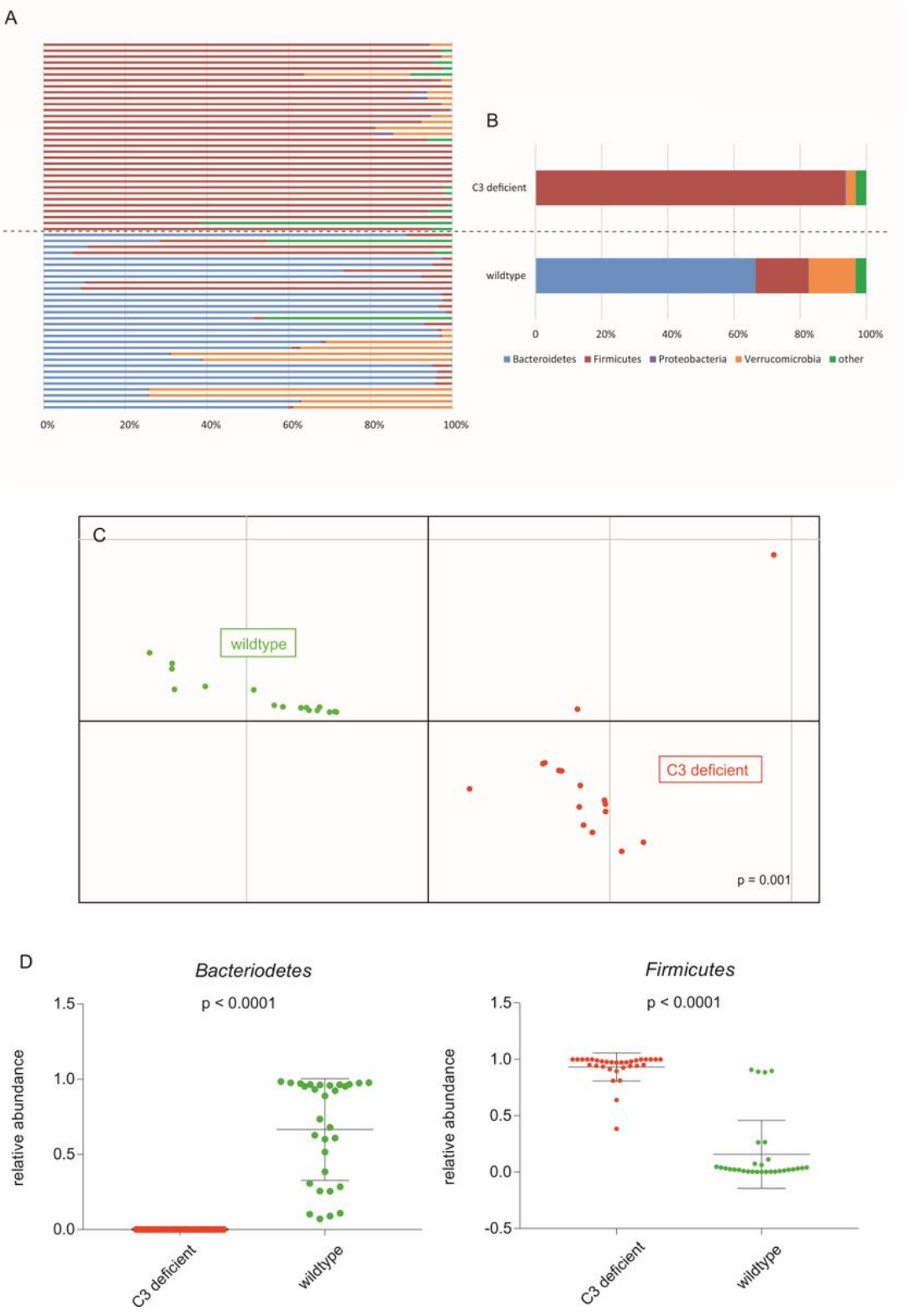

Figure 4

Diversity of the intestinal microbiome in C3 deficient mice and wildtypes. Relative abundances of microbiota at phyla level in all mice (a) and averaged for groups (b). c: Principal component analysis of microbial species abundance grouped C3 deficient mice and wildtypes separately, with PERMANOVA confirming a significant difference between the groups ($p = 0.001$). Representative data of one experiment is shown. d: Relative abundances of taxa associated with C3 deficiency (Wilcoxon rank sum test, $p < 0.05$).